# Low-symmetric quantum magnets as a step to terahertz invisibility

A. A. Zvyagin[1,2,3,*] and V. V. Slavin[1]

[1]*B. Verkin Institute for Low Temperature Physics and Engineering of the National Academy of Sciences of Ukraine, Nauky Ave., 47, Kharkiv 61103, Ukraine*

[2]*Max-Planck-Institut für Physik komplexer Systeme, Nöthnitzer Str. 38, D-01187 Dresden, Germany*

[3]*V.N. Karazin Kharkiv National University, Svobody sq., 4, Kharkiv 61002, Ukraine*

(Received 25 April 2025; revised 4 January 2026; accepted 22 January 2026; published 17 February 2026)

Quantum spin systems with low symmetries of the magnetic properties are studied. It is shown that the low symmetry yields special effects of their magnetic characteristics. Magnetic moments induced by the external magnetic field can be nonparallel to the direction of the field. Also, components of the magnetic susceptibility of such systems can be negative in a large range of the field and temperature values, i.e., they manifest diamagnetic behavior. The origin of the effect is totally quantum. Such a behavior is generic for quantum paramagnets, low-dimensional quantum spin systems, and for quantum spin systems with geometrical frustration of spin-spin couplings. The effect can be important for applications of such quantum systems, e.g., in the creation of metamaterials or in quantum computing.

DOI: 10.1103/ch7p-gfg9

## I. INTRODUCTION

Magnetic systems often reveal anisotropic properties [1]. In magnetically ordered systems, the magnetic anisotropy is the reason for the onset of the metamagnetism, spin-flop transitions, weak ferromagnetism, etc. [2]. The magnetic anisotropy in crystals is the manifestation of symmetries in positions of magnetic ions and nonmagnetic ones (ligands) [3]. For single magnetic ions, the crystalline electric field of ligands acts on orbital moments of magnetic ions and, due to the spin-orbit coupling, produces anisotropic properties of the latter. On the other hand, the indirect exchange between magnetic ions also depends on the orbital anisotropy of participating ligands. Finally, the magnetic dipole-dipole interaction depends on the orientation of magnetic ions in crystals. This is why, despite the relativistic origin of the magnetic anisotropy, the latter can dramatically change properties of magnets, especially of quantum ones [4]. For paramagnetic ions, the magnetic anisotropy is manifested in anisotropic effective $g$ factors and in the onset of spin (for transition metal ions) or total moment (for rare-earth ions) multipole operators in the Hamiltonian. The latter exists only for values of spins or total moments of the localized electrons larger or equal to one. For many-body quantum spin systems, one can introduce intersite quadrupole moments, which can exist even for spins 1/2 [5]. The important feature of quadrupole moments is their linear coupling to the external electric field [6] or strains [7], which permits us to regulate the anisotropy in magnetic systems.

Despite numerous realizations of crystal symmetries in magnets, researchers often concentrated on studies of properties of highly symmetric magnetic systems like cubic, hexagonal, or tetragonal ones [8]. However, properties of low-symmetric magnetic systems can manifest very important properties, which are absent in their highly symmetric counterparts. In this contribution, we study interesting properties of quantum spin systems with low magnetic symmetries. We show that such systems manifest special features in their magnetic behavior. Namely, we show that the low-symmetric magnetic anisotropy can yield the onset of magnetic moments of quantum spins nonparallel to the direction of the applied magnetic field. Those magnetic moments, unlike the ones for magnetically ordered systems, manifest the nonmonotonic behavior as a function of applied field. One can observe the negative magnetic susceptibility (i.e., the decrease of the absolute value of the magnetic moment with the growth of the magnetic field), characteristic for diamagnets [1]. That phenomenon has no analogies in magnetically ordered systems. We show that it exists for single-ion paramagnets, one- and two-dimensional magnetically disordered spin systems, and in three-dimensional quantum spin systems with the geometric frustration of spin-spin couplings [9–12] (collective paramagnets [13]). That peculiar magnetic field behavior of quantum spin systems can be important in such modern regions of research as studies of metamaterials (where negative susceptibilities play the crucial role) or in quantum computing (where low symmetries of distribution of qubits or qudits and their environment can yield special features of their response to gates [14,15]). One of the promising areas of application of such magnetic compounds is the design of new $\mu$-negative metamaterials [16–24]. In those compounds a negative refractive index for electromagnetic waves is caused by the negative value of magnetic permittivity $\mu$. Today, one of the most important problems is to create metamaterials in which the negative index is retained at least up to the terahertz (THz) range. Preliminary estimates show that this requirement is met

*Contact author: dr.zvyagin@gmail.com

*Published by the American Physical Society under the terms of the Creative Commons Attribution 4.0 International license. Further distribution of this work must maintain attribution to the author(s) and the published article's title, journal citation, and DOI. Open access publication funded by Max Planck Society.*

for low-symmetry magnets based on rare-earth ions. Another interesting direction of studies is related to the development of magnetic gates for spin-based qubits [25–27]. Also, since the appearance of the transverse component of the magnetic moment affects the entanglement of the quantum states of quibits [28], the considered phenomena can be used for the design of different gates for quantum computations.

## II. SINGLE-ION PARAMAGNETS

To set the stage, let us start with the consideration of the Hamiltonian of the simplest quantum magnetic system with an anisotropy: the quantum paramagnet. We study magnetic ions with $3d$ (transition metal elements) or $4f$ (rare-earth elements). For transition metals, the energy of the spin-orbit coupling for localized electrons (of the order of $10^2$–$10^3$ K) is smaller than the energy of the crystalline electric field of ligands ($10^3$–$10^4$ K), and the total orbital moment $L$ and the total spin $S$ of the electron configuration are good quantum numbers. On the other hand, for rare-earth elements, the energy of the crystalline electric field is larger than the one of the spin-orbit coupling, and the total moment $J$ is a good quantum number. Neglecting hyperfine interactions between magnetic moments of electrons and nuclei (of the order of $10^{-1}$–$10^{-2}$ K) and weak spin-spin couplings (e.g., the magnetic dipole-dipole interaction with the energy of the order of 1 K or smaller), we can consider the Hamiltonian of the quantum paramagnet with the transition metal ion as [29]

$$\mathcal{H}_p = \sum_{n=2,4,6}\sum_{m=1}^{n} a_{nm}x_n\left[B_n^m\left(O_n^m\right)_p + C_n^m\left(\Omega_n^m\right)_p\right] - \mu_B\sum_{i=x,y,z} g_i H_i S_p^i, \tag{1}$$

where $p$ defines the site of the lattice, $B_n^m$ and $C_n^m$ are the values of the crystalline electric field, $(O_n^m)_p$ and $(\Omega_n^m)_p$ are equivalent Stevens operators (related to $S_p^i$) [29], $S_p^i$ are the operators of the projections of the total spin of the lowest-energy electron configuration, $\mu_B$ is the Bohr magneton, $g_i$ are effective $g$ factors, $H_i$ are the components of the external magnetic field, $a_{nm}$ are the proportionality coefficients between the Stevens operators and spherical functions [30], and $x_n = \alpha, \beta$ (for rare-earth ions, one has $x_n = \alpha_J, \beta_J, \gamma_J$) are the Stevens coefficients [29]. In fact, Stevens operators are the operators of multipole moments. For rare-earth ions, we must replace operators of the spin projections by the ones of the total moment (also in the definitions of Stevens operators). Here, we also neglect nonlinear interaction of spins (total moments) with the external magnetic field, i.e., terms with odd $n$ for Stevens operators. In the following formulas, we define $h_i = \mu_B g_i H_i$ and use the units in which $a_{nm} = x_n = 1$ for brevity.

In this study, we consider magnetic ions with a low symmetry of the nonmagnetic ligands, surrounding the magnetic ion. To illustrate the effect, we look at the situation of the monoclinic symmetry for $S = 3/2$, with only nonzero values of the crystalline electric field $B_2^2$ and $C_2^2$ and with nonzero $i = x, y$ components of the external magnetic field. The partition function of the system can be written as (for brevity, we use $\alpha = \beta = a_{22} = 1$)

$$Z = 2\cosh\left(\frac{\varepsilon_1}{2k_BT}\right) + 2\cosh\left(\frac{\varepsilon_2}{2k_BT}\right), \tag{2}$$

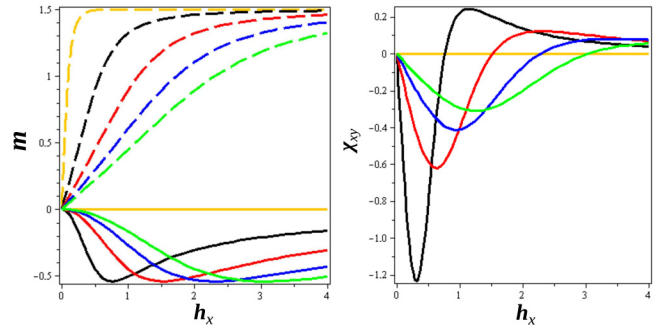



FIG. 1. Left panel: The dependence of the $x$ projection of the magnetic moment $m^x = M^x/g_x\mu_B$ (dashed lines) and the $y$ projection $m^y$ (solid lines) of the monoclinic quantum $S = 3/2$ paramagnet on the external magnetic field $h_x = H_x/g_x\mu_B$ ($H_y = 0$) and several values of the crystalline electric field $C_2^2$ (orange $C_2^2 = 0$, black $C_2^2 = 0.5$, red $C_2^2 = 1$, blue $C_2^2 = 1.5$, and green $C_2^2 = 2$) for $B_2^2 = 0$ and $T = 0.1$ ($k_B = 1$). Right panel: The dependence of the magnetic susceptibility $X_{xy} = \chi_{xy}/g_x g_y \mu_B^2$ on the magnetic field $h_x$.

where $T$ is the temperature, $k_B$ is the Boltzmann constant, and

$$\varepsilon_{1,2} = \left\{5\left(h_x^2 + h_y^2\right) + 6\left[\left(B_2^2\right)^2 + \left(C_2^2\right)^2\right] \pm 2F\right\}^{1/2},$$
$$F = \left\{4\left(h_x^2 + h_y^2\right)^2 + 3\left(h_x^2 + h_y^2\right)\left[\left(B_2^2\right)^2 + \left(C_2^2\right)^2\right] + 9\left[\left(B_2^2\right)^2 + \left(C_2^2\right)^2\right]^2 + 6\sqrt{3}\left[h_y^3 C_2^2 - h_x^3 B_2^2 + 3h_x h_y\left(h_y B_2^2 - h_x C_2^2\right)\right]\right\}^{1/2}. \tag{3}$$

Then using the standard laws of thermodynamics, we obtain for the components of the magnetic moment

$$M^{x,y} = \frac{g_{x,y}\mu_B}{Z}\sum_{i=1,2}\frac{y_i^{x,y}\sinh\left(\frac{\varepsilon_i}{2k_BT}\right)}{\varepsilon_i}, \tag{4}$$

where

$$y_{1,2}^x = 5h_x \pm \frac{2}{F}\left\{4\left(h_x^2 + h_y^2\right)h_x + 3\left[\left(B_2^2\right)^2 + \left(C_2^2\right)^2\right]h_x + 9\sqrt{3}\left[B_2^2\left(h_y^2 - h_x^2\right) - 2h_x h_y C_2^2\right]\right\},$$
$$y_{1,2}^y = 5h_y \pm \frac{2}{F}\left\{4\left(h_x^2 + h_y^2\right)h_y + 3\left[\left(B_2^2\right)^2 + \left(C_2^2\right)^2\right]h_y + 9\sqrt{3}\left[C_2^2\left(h_y^2 - h_x^2\right) + 2h_x h_y B_2^2\right]\right\}. \tag{5}$$

It is easy to see that, for $H_x = 0$, one has $M^y(H_y) \neq 0$ (the trivial situation) but with $M^x(H_y) \neq 0$. Vice versa, for $H_y = 0$, one has $M^x(H_x) \neq 0$ and $M^y(H_x) \neq 0$. It means that the monoclinic magnetic anisotropy of ligands yields, together with the nonzero projections of magnetic moments of the quantum paramagnet parallel to the direction of the external magnetic field, nonzero contribution to the magnetic moments with components perpendicular to the direction of the magnetic field. As it must be for $H_{x,y} = 0$, the value of the magnetic moment of the quantum paramagnet is zero. For $H_x = 0$, the effect is related to the nonzero component of the crystalline electric field $B_2^2$ and, for $H_y = 0$, to nonzero $C_2^2$. The behavior of the components of the magnetic moments and susceptibilities $\chi_{ij} = \partial M^i/\partial H_j$ for such a quantum paramagnet are illustrated for $T = 0.1$ ($k_B = 1$) and $B_2^2 = 0$ in Fig. 1 and, for $C_2^2 = 0$, in Fig. 2.

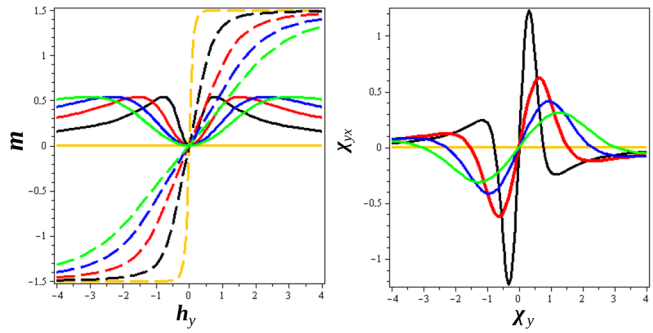



FIG. 2. Left panel: The dependence of the $x$ projection of the magnetic moment $m^x$ (dashed lines) and the $y$ projection $m^y$ (solid lines) of the monoclinic quantum $S = 3/2$ paramagnet on the external magnetic field $h_y$ ($H_x = 0$) and several values of the crystalline electric field $B_2^2$ (orange $B_2^2 = 0$, black $B_2^2 = 0.5$, red $B_2^2 = 1$, blue $B_2^2 = 1.5$, and green $B_2^2 = 2$) for $C_2^2 = 0$ and $T = 0.1$ ($k_B = 1$). Right panel: The dependence of the magnetic susceptibility $X_{yx} = \chi_{yx}/g_x g_y \mu_B^2$ on the magnetic field $h_y$.

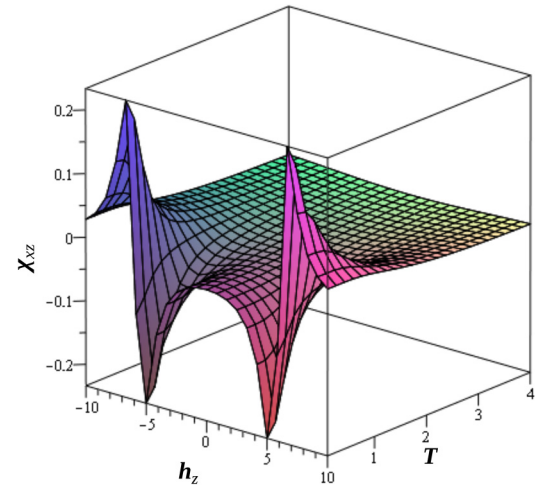



FIG. 3. The dependence of the magnetic susceptibility $X_{xz} = \chi_{xz}/g_x g_z \mu_B^2$ on the magnetic field $h_z = g_z \mu_B H_z$ and temperature $T$ ($k_B = 1$) of the spin $S = 1$ triclinic paramagnet with $a_{2m}\alpha = 1$, $B_2^0 = 2$, $B_2^1 = 0.5$, $C_2^1 = 0.3$, $B_2^2 = 1$, and $C_2^2 = 0.2$.

We point out that the value $(m^x)^2 + (m^y)^2 + (m^z)^2$ can be larger than $S^2 = 9/4$, but it is always smaller or equal to $S(S+1) = 15/4$, as it must be for quantum systems. Notice that, for the longitudinal response, $M^{x,y}(H_{x,y}) = -M^{x,y}(-H_{x,y})$ for zero values of other projections of the magnetic field $H_{y,x} = 0$ and for $B_2^2 = 0$ and $C_2^2 = 0$, respectively. For the components of the magnetic moment, induced by the perpendicularly directed magnetic field, we have $M^x(C_2^2, H_y) = -M^x(-C_2^2, H_y)$ for $H_y = 0$ and $B_2^2 = 0$ and $M^y(B_2^2, H_x) = M^x(-B_2^2, H_x)$ for $C_2^2 = 0$ and $H_x = 0$. On the other hand, for the components of the magnetic moment, induced by the nonparallel magnetic field, for both nonzero components of the crystalline electric field or external magnetic field, there are no such symmetries. Notice that, depending on the sign of the crystalline electric fields $B_2^2$ and $C_2^2$, perpendicular to the direction of the applied magnetic field moment can be positive or negative. Also, it turns out that such a moment depends on the applied field nonmonotonically. Its absolute value can first increase with the growth of the field value and then decrease. The decrease of the magnetic moment with the growth of the applied field implies a negative value of the related component of the magnetic susceptibility.

In Fig. 3 we show the temperature and magnetic field behavior of the magnetic susceptibility of the spin $S = 1$ triclinic paramagnet. One can clearly see that there exists a wide region of values of the magnetic field and temperature in which the component of the magnetic susceptibility is negative. The important feature of the triclinic $S = 3/2$ paramagnet, comparing with the $S = 1$ case, see the next subsection, is the presence of regions of the values of the temperature and magnetic field, at which the absolute value of the magnetic moment decreases with the growth of the field, for the magnetic moment directed parallel to the magnetic field, i.e., of the negative magnetic susceptibility. The negative magnetic susceptibility is characteristic for diamagnets.

For the general case of the triclinic symmetry for $S = 1$ and $3/2$, we present some details of analytic calculation and results in the next subsection.

### A. Magnetic moments of the triclinic paramagnet

The Hamiltonian of the spin-1 and 3/2 triclinic paramagnet is

$$\mathcal{H}_p = \sum_{m=0}^{2} \left[\tilde{B}_2^m \left(O_2^n\right)_p + \tilde{C}_2^n \left(\Omega_2^m\right)_p\right] - \mu_B \sum_{i=x,y,z} g_i H_i S_p^i, \quad (6)$$

where we denote $\tilde{B}_2^m = a_{2m}\alpha B_2^m$ and $\tilde{C}_2^m = a_{2m}\alpha C_2^m$. The eigenvalues of the Hamiltonian in Eq. (6) for $S = 1$ are

$$\varepsilon_1 = u + v, \quad \varepsilon_{2,3} = -\frac{u+v}{2} \pm i\sqrt{3}\frac{u-v}{2}, \quad (7)$$

where

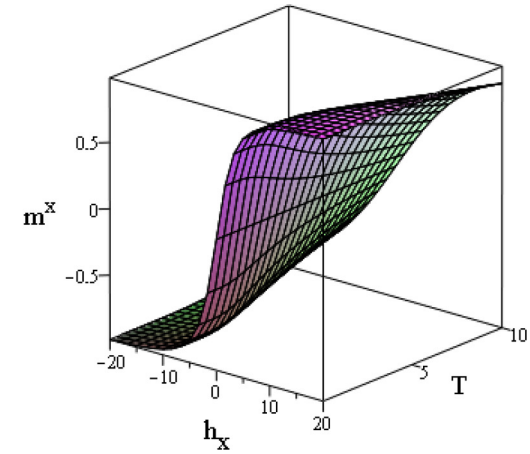
$$u = \left(-\frac{t}{2} + \sqrt{d}\right)^{1/3}, \quad v = \left(-\frac{t}{2} - \sqrt{d}\right)^{1/3},$$
$$d = \left(\frac{s}{3}\right)^3 + \left(\frac{t}{2}\right)^2. \quad (8)$$

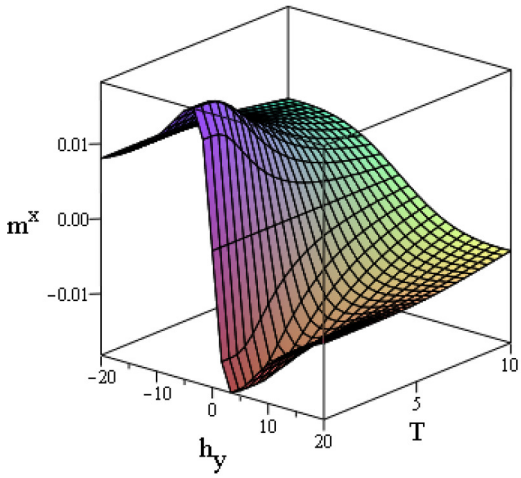
Here, we denote

$$\begin{aligned} s = & -3\left(\tilde{B}_2^0\right)^2 - \left(\tilde{B}_2^1\right)^2 - \left(\tilde{B}_2^2\right)^2 - \left(\tilde{C}_2^1\right)^2 - \left(\tilde{C}_2^2\right)^2 \\ & - (g_x\mu_B H_x)^2 - (g_y\mu_B H_y)^2 - (g_z\mu_B H_z)^2, \\ t = & \tilde{B}_2^0\left[\left(\tilde{B}_2^1\right)^2 + \left(\tilde{C}_2^1\right)^2 + (g_x\mu_B H_x)^2 + (g_y\mu_B H_y)^2\right] \\ & - 2\tilde{B}_2^0\left[\left(\tilde{B}_2^2\right)^2 + \left(\tilde{C}_2^2\right)^2 + (g_z\mu_B H_z)^2\right] \\ & + \tilde{B}_2^2\left[\left(\tilde{B}_2^1\right)^2 - \left(\tilde{C}_2^1\right)^2 - (g_x\mu_B H_x)^2 + (g_y\mu_B H_y)^2\right] \\ & - 2g_z\mu_B H_z\left[\tilde{B}_2^1 g_x\mu_B H_x + \tilde{C}_2^1 g_y\mu_B H_y\right] \\ & + 2\tilde{C}_2^2\left[\tilde{B}_2^1\tilde{C}_2^1 - g_x g_y \mu_B^2 H_x H_y\right]. \end{aligned}$$

Then as usual, the partition function is

$$\begin{aligned} Z &= \sum_{i=1}^{3} \exp(-\varepsilon_i/k_B T) \\ &= \exp[-(u+v)/k_B T] + 2\exp[(u+v)/2k_B T] \\ &\quad \times \cos[\sqrt{3}(u-v)/2k_B T], \end{aligned} \quad (9)$$



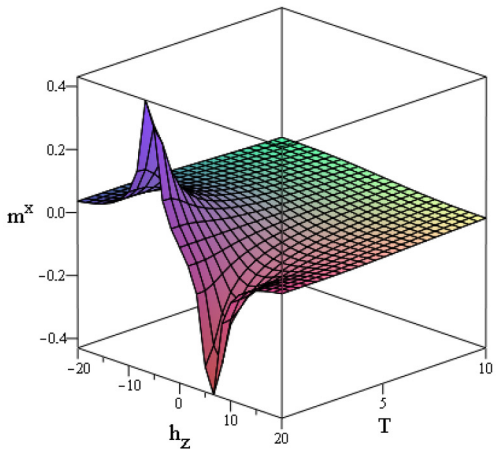
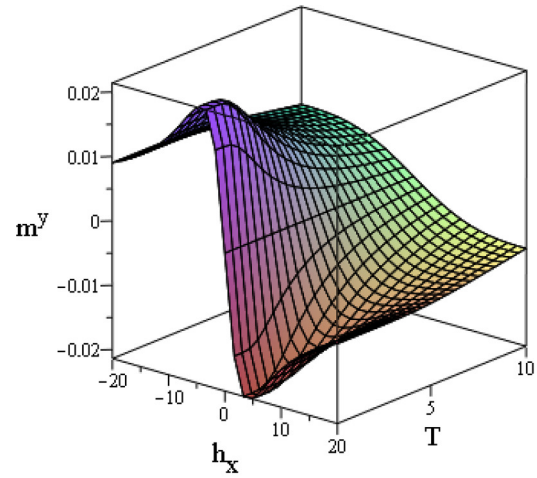
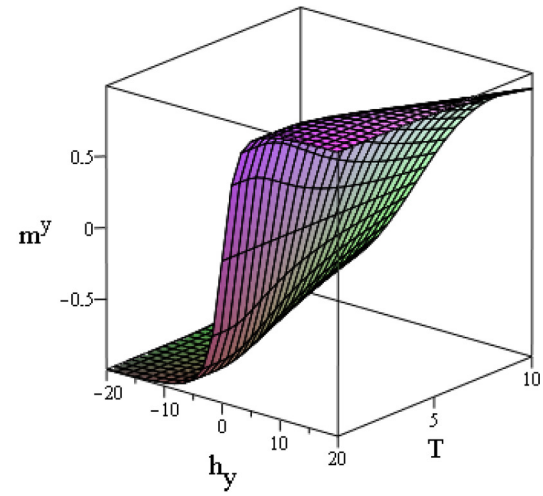




FIG. 4. Upper panel: The dependence of the $x$ projection of the magnetic moment $m^x = M^x/g_x\mu_B$ of the triclinic quantum $S = 1$ paramagnet as a function of the external magnetic field $h_x = g_x\mu_B H_x$ ($H_y = H_z = 0$) and the temperature $T$. Middle panel: The same for the external magnetic field $h_y = g_y\mu_B H_y$ ($H_x = H_z = 0$). Lower panel: The same for the external magnetic field $h_z = g_z\mu_B H_z$ ($H_x = H_y = 0$).



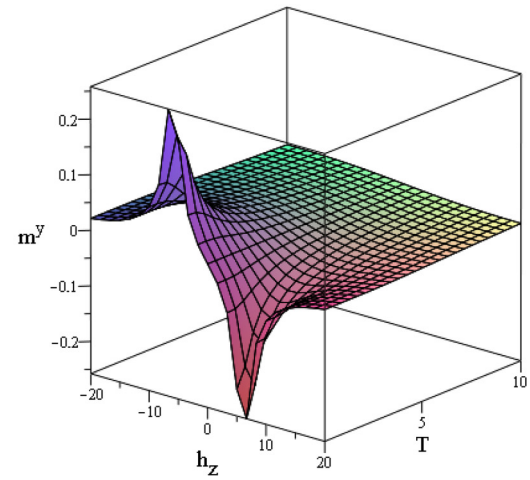




FIG. 5. Upper panel: The dependence of the $y$ projection of the magnetic moment $m^y = M^y/g_y\mu_B$ of the triclinic quantum $S = 1$ paramagnet as a function of the external magnetic field $h_x = g_x\mu_B H_x$ ($H_y = H_z = 0$) and the temperature $T$. Middle panel: The same for the external magnetic field $h_y = g_y\mu_B H_y$ ($H_x = H_z = 0$). Lower panel: The same for the external magnetic field $h_z = g_z\mu_B H_z$ ($H_x = H_y = 0$).

where $k_B$ is the Boltzmann constant, and $T$ is the temperature. The free energy of the triclinic spin-1 paramagnet is then $f = -k_B T \ln(Z)$. Calculation of the expectation values of the operators of projections of the spin and quadrupole moments and their derivatives are then obvious.

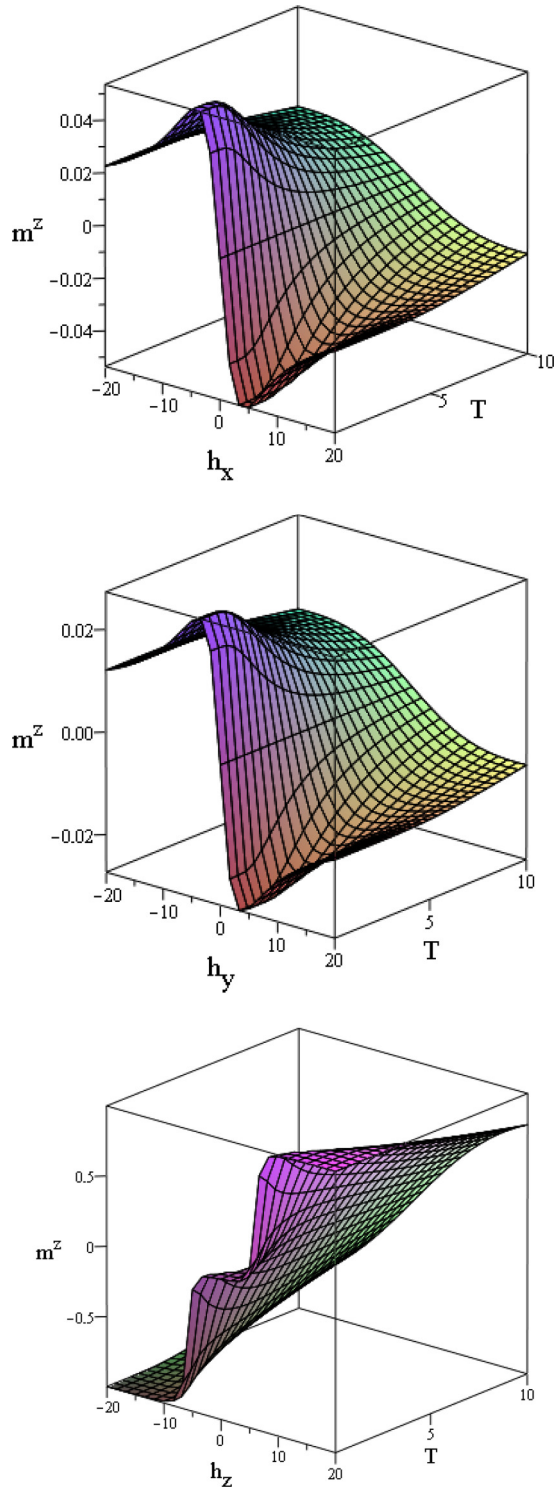



FIG. 6. Upper panel: The dependence of the $z$ projection of the magnetic moment $m^z = M^z/g_z\mu_B$ of the triclinic quantum $S = 1$ paramagnet as a function of the external magnetic field $h_x = g_x\mu_B H_x$ ($H_y = H_z = 0$) and the temperature $T$. Middle panel: The same for the external magnetic field $h_y = g_y\mu_B H_y$ ($H_x = H_z = 0$). Lower panel: The same for the external magnetic field $h_z = g_z\mu_B H_z$ ($H_x = H_y = 0$).

In the following Figs. 4–6, we present the results of calculations of the magnetic field and temperature dependences of magnetic moments of the triclinic spin-1 paramagnet. In

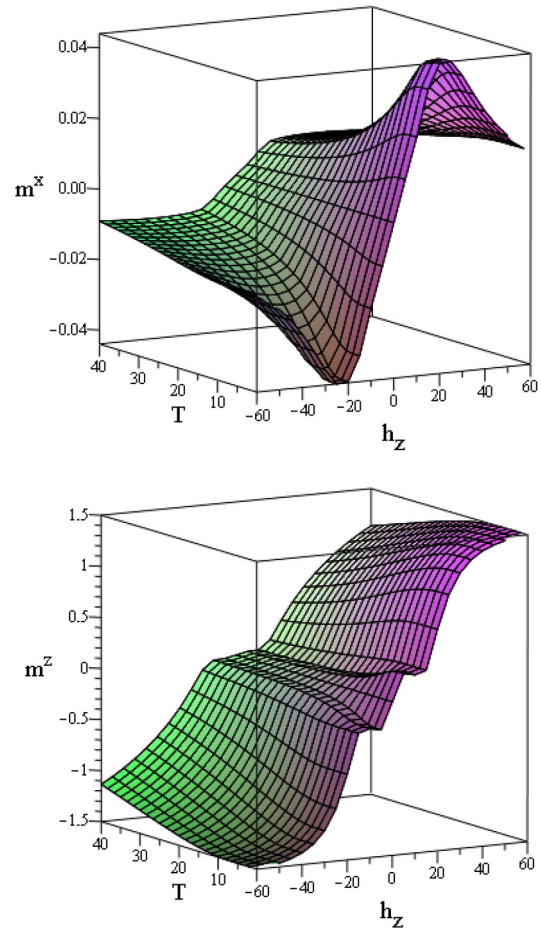



FIG. 7. Upper panel: The dependence of the $x$ projection of the magnetic moment $m^x = M^x/g_x\mu_B$ of the triclinic quantum $S = 3/2$ paramagnet as a function of the external magnetic field $h_z = g_z\mu_B H_z$ ($H_y = H_x = 0$) and the temperature $T$. Lower panel: The same for the $z$ projection of the magnetic moment $m^z = M^z/g_z\mu_B$.

our calculations, we use the following parameters: $a_{2m}\alpha = 1$, $B_2^0 = 2$, $B_2^1 = 0.5$, $C_2^1 = 0.3$, $B_2^2 = 1$, $C_2^2 = 0.2$, and units in which $k_B = 1$.

For $S = 3/2$, it is also possible to calculate analytically thermodynamic characteristics of the triclinic paramagnet. Using the same values of parameters as for the case $S = 1$, we obtain the results for the magnetic field and temperature dependencies of the projections of the magnetic moments, presented in Fig. 7.

One can again see that the triclinic crystalline electric fields cause nonzero magnetic moments directed perpendicular to the external magnetic field. For spin $S = 3/2$, the scales for essential changes of the magnetic moments with $T$ and the magnetic field are larger than for $S = 1$. Again, there exist regions of values of the temperature and magnetic field at which the absolute value of the magnetic moment decreases with the growth of the field, i.e., with negative magnetic susceptibility. The important feature of the triclinic $S = 3/2$ paramagnet, comparing with the $S = 1$ case, is the presence of regions of values of the temperature and magnetic field at which the absolute value of the magnetic moment decreases with the growth of the field, for the magnetic moment directed parallel

TABLE I. Components of the crystalline electric field and related local symmetry groups which yield nonzero magnetic moments of the paramagnetic transition metal and rare-earth ions caused by the magnetic field directed perpendicular.

| $B_n^m, C_n^m > 0$ | $h_x$ | $h_y$ | $h_z$ | Symmetry group |
|---|---|---|---|---|
| $B_2^1$ | $m^z < 0$ | – | $m^x < 0$ | $C_1, C_i(S_2)$ |
| $C_2^1$ | – | $m^z > 0$ | $m^y < 0$ | $C_1, C_i(S_2)$ |
| $B_2^2$ | – | $m^x > 0$ | – | $C_2, C_s(C_{1h}), C_{2h}$ |
| $(S = 3/2)$ | | | | $D_2, C_{2v}, D_{2h}$ |
| $C_2^2$ | $m^y < 0$ | $m^x < 0$ | – | $C_1, C_i(S_2)$, |
| | | | | $C_2, C_s(C_{1h}), C_{2h}$ |
| $B_4^1$ | $m^z < 0$ | – | $m^x < 0$ | $C_1, C_i(S_2)$ |
| $C_4^1$ | – | $m^z < 0$ | $m^y < 0$ | $C_1, C_i(S_2)$ |
| $C_4^2$ | $m^y < 0$ | $m^x < 0$ | – | $C_2, C_s(C_{1h}), C_{2h}$ |
| $B_4^3$ | $m^z < 0$ | – | – | $C_1, C_i(S_2)$ |
| | | | | $D_3, C_{3v}, D_{3d}$ |
| $C_4^3$ | – | $m^z > 0$ | – | $C_1, C_i(S_2)$ |
| | | | | $C_3, C_{3i}(S_6)$ |
| $C_4^4$ | $m^y < 0$ | $m^x > 0$ | – | $C_1, C_i(S_2)$ |
| | | | | $C_2, C_2(C_{1h}), C_{2h}$ |
| | | | | $C_4, S_4, C_{4h}$ |

TABLE II. Components of the crystalline electric field and related local symmetry groups which yield nonzero magnetic moments of the paramagnetic rare-earth ions caused by the magnetic field directed perpendicular.

| $B_n^m, C_n^m > 0$ | $h_x$ | $h_y$ | $h_z$ | Symmetry group |
|---|---|---|---|---|
| $C_6^2$ | $m^y < 0$ | $m^z < 0$ | – | $C_1, C_i(S_2)$ |
| | | | | $C_2, C_2(C_{1h}), C_{2h}$ |
| $B_6^3$ | $m^z > 0$ | – | – | $C_1, C_i(S_2)$ |
| | | | | $C_3, C_{3i}(S_6)$ |
| $C_6^3$ | – | $m^z < 0$ | – | $C_1, C_i(S_2)$ |
| | | | | $C_3, C_{3i}(S_6)$ |
| $C_6^4$ | $m^y > 0$ | $m^x < 0$ | – | $C_1, C_i(S_2)$ |
| | | | – | $C_2, C_s(C_{1h}), C_{2h}$ |
| | | | – | $C_4, S_4, C_{4h}$ |
| $B_6^5$ | $m^z < 0$ | – | – | $C_1, C_i(S_2)$ |
| $C_6^5$ | – | $m^z < 0$ | – | $C_1, C_i(S_2)$ |
| $C_6^6$ | $m^y < 0$ | $m^x < 0$ | – | $C_1, C_i(S_2)$ |
| | | | | $C_2, C_s(C_{1h}), C_{2h}$ |
| | | | | $C_3, C_{3i}(S_6)$ |
| | | | | $C_4, S_4, C_{4h}$ |

to the magnetic field. The magnetic field and temperature behavior of components of the magnetic moments reflects the symmetry properties of the triclinic paramagnet.

### B. General case: Symmetries of ligands

The results for the behavior of magnetic moments for quantum paramagnets with different types of symmetries of nonmagnetic ligands are presented in Tables I and II. The Stevens operators, related to the crystalline electric fields presented in Tables I and II, are shown below. The groups $C_1$ and $C_i(S_2)$ belong to the triclinic symmetry; $C_2$, $C_s(C_{1h})$ and $C_{2h}$ belong to the monoclinic symmetry; $D_2$, $C_{2v}$, and $D_{2h}$ to the orthorhombic one; $D_3, C_{3v}, D_{3d}, C_3$, and $C_{3i}(S_6)$ to the trigonal one; $C_4$, $S_4$, and $C_{4h}$ to the tetragonal one; and the groups $C_6$, $C_{3h}$, and $C_{6h}$ belong to the hexagonal symmetry.

Here, we present the Stevens operators from Tables I and II, which produce nonzero magnetic moment nonparallel to the applied magnetic field. For the total moments $J$, those operators are (here, $J_\pm = J_x \pm iJ_y$)

$$
\begin{aligned}
&O_2^1 = \frac{1}{4}(J_zJ_+ + J_+J_z + J_zJ_- + J_-J_z)\,, \quad \Omega_2^1 = \frac{1}{4i}(J_zJ_+ + J_+J_z - J_zJ_- - J_-J_z)\,, \quad O_2^2 = \frac{1}{2}(J_+^2 + J_-^2),\\
&\Omega_2^2 = \frac{1}{2i}(J_+^2 - J_-^2)\,, \quad O_4^1 = \frac{1}{4}[([7J_z^3 - 3J(J+1)+1]J_z)J_+ + J_+([7J_z^3 - 3J(J+1)+1]J_z)\\
&\quad + ([7J_z^3 - 3J(J+1)+1]J_z)J_- + J_-([7J_z^3 - 3J(J+1)+1]J_z)]\,,\\
&\Omega_4^1 = \frac{1}{4i}[([7J_z^3 - 3J(J+1)+1]J_z)J_+ + J_+([7J_z^3 - 3J(J+1)+1]J_z) - ([7J_z^3 - 3J(J+1)+1]J_z)J_-\\
&\quad - J_-([7J_z^3 - 3J(J+1)+1]J_z)]\,,\\
&\Omega_4^2 = \frac{1}{4i}[(7J_z^2 - J(J+1) - 5)J_+^2 + J_+^2(7J_z^2 - J(J+1) - 5) - (7J_z^2 - J(J+1) - 5)J_-^2 - J_-^2(7J_z^2 - J(J+1) - 5)]\,,\\
&O_4^3 = \frac{1}{4}[J_z(J_+^3 + J_-^3) + (J_+^3 + J_-^3)J_z]\,, \quad \Omega_4^3 = \frac{1}{4i}[J_z(J_+^3 - J_-^3) + (J_+^3 - J_-^3)J_z]\,, \quad \Omega_4^4 = \frac{1}{2i}(J_+^4 - J_-^4)\,,
\end{aligned}
\tag{10}
$$

$$
\begin{aligned}
\Omega_6^2 = \frac{1}{4i}[&(33J_z^4 - [18J(J+1)+123]J_z^2 + J^2(J+1)^2 + 10J(J+1) + 102)J_+^2\\
&+ J_+^2(33J_z^4 - [18J(J+1)+123]J_z^2 + J^2(J+1)^2 + 10J(J+1) + 102)\\
&- (33J_z^4 - [18J(J+1)+123]J_z^2 + J^2(J+1)^2 + 10J(J+1) + 102)J_-^2\\
&- J_-^2(33J_z^4 - [18J(J+1)+123]J_z^2 + J^2(J+1)^2 + 10J(J+1) + 102)]\,,\\
\Omega_6^3 = \frac{1}{4i}[&(11J_z^3 - [3J(J+1)+59]J_z)J_+^3 + J_+^3(11J_z^3 - [3J(J+1)+59]J_z)\\
&- (11J_z^3 - [3J(J+1)+59]J_z)J_-^3 - J_-^3(11J_z^3 - [3J(J+1)+59]J_z)]
\end{aligned}
$$

$$O_6^5 = \frac{1}{4}[J_z J_+^5 + J_+^5 J_z + J_z J_-^5 + J_-^5 J_z]\,, \quad \Omega_6^5 = \frac{1}{4i}[J_z J_+^5 + J_+^5 J_z - J_z J_-^5 - J_-^5 J_z]\,,$$
$$\Omega_6^6 = \frac{1}{2i}(J_+^6 - J_-^6)\,. \tag{11}$$

For spins, one has to replace $J \to S$ and $J_{z,\pm} \to S_{z,\pm}$ with $S_\pm = S_x \pm iS_y$.

The effect due to the presence of non-negative components of the crystalline electric field for higher spin (total moment) values is similar to the one shown in Figs. 1–7. However, the values of the changes of the components of the magnetic moment, cased by the perpendicular magnetic field, are smaller for larger values of $S$ for ions of transition metals or $J$ for rare-earth ions.

We emphasize that the effect implies nonzero values of the nondiagonal components of the magnetic susceptibility tensor $\chi_{ij}$ ($i \neq j$, $i, j = x, y, z$). The important point is that the components of the magnetic susceptibility can become negative. Their negativity depends on the signs of the related crystalline electric fields and on the value of the applied magnetic field. Negative values of the components of the magnetic susceptibility tensor appear in a similar way as shown in Figs. 1–7, i.e., for those values of the magnetic field and temperature at which the absolute values of the projections of magnetic moments decrease with the growth of the magnetic field. Values of the crystalline electric field can be changed by strains or (for the noncentrosymmetric case) by the application of the external electric field. Hence, one can obtain the negative magnetic susceptibility by governing its onset by external parameters. Negative magnetic susceptibility (for positive electric one) means the negative total electromagnetic susceptibility of the system. The effect of the latter is widely used in modern metamaterials.

## III. PARAMAGNETS WITH SPIN-SPIN INTERACTIONS

Such a behavior of magnetic characteristics of quantum paramagnets exists also for spin chains, spin planes, and three-dimensional spin systems with the geometric frustration of spin-spin couplings (quantum spin ices [9–12,31]) with a low symmetric anisotropy of the couplings.

The general Hamiltonian of the considered quantum spin system is $\mathcal{H} = \sum_p \mathcal{H}_p + \mathcal{H}_{\rm int}$ with the interaction part of the Hamiltonian being

$$\mathcal{H}_{\rm int} = \sum_{p,q} \sum_{i,j=x,y,z} J_{ij} S_p^i S_q^j, \tag{12}$$

where $p, q$ denote the coordinates of (nearest-neighbor) spins in the system, and $J_{ij}$ are coupling parameters. Obviously, for quantum spin systems without magnetic ordering for higher values of spins, the single-ion anisotropy matters, and hence, the aforementioned effects, are present for the low symmetry of ligands. We point out that, namely, the terms like $S_p^i S_q^j + S_p^j S_q^i$, with $i, j = x, y, z$, $i \neq j$, in the interacting part of the Hamiltonian produce nonzero magnetic moments as the response to the nonparallel magnetic field.

Zero-temperature field dependencies of the magnetic moment for finite-size chains with $S = 1/2$ and monoclinic anisotropy of the exchange are presented in Fig. 8. The left and right panels illustrate how the effect depends on the value of $J_{xy} = J_{yx}$, see Eq. (12). Similar effects appear for $J_{xz} = J_{zx}$ and $J_{yz} = J_{zy}$ for the respected directions of the applied magnetic field.

In Fig. 9, similar dependencies for the one-dimensional chain but for finite temperatures are presented. The left panel corresponds to $J_{xy} = 0.1$; the right panel corresponds to $J_{xy} = 0.5$.

In Fig. 10, similar dependencies for two-dimensional square lattices are presented. The left panel corresponds to a $4 \times 2$ lattice and finite temperatures. The right panel corresponds to a $4 \times 4$ lattice and $T = 0$.

Figure 11 demonstrates field dependencies of the magnetic moment of a single tetrahedron with $N = 4$ spins at finite temperatures (the left panel) and zero-temperature dependencies of the cluster of $4 \times$ tetrahedrons with $N = 16$ spins (the right panel).

Again, in the regions where absolute values of magnetic moments decrease with the growth of the magnetic field, the

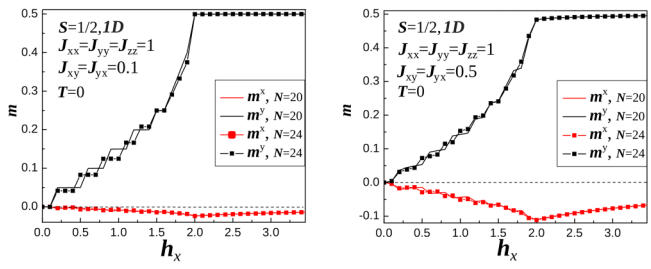



FIG. 8. Spin $S = 1/2$ chain. The dependencies of the magnetic moments $m^x$ (black curves) and $m^y$ (red curves) on the magnetic filed $h_x$. We use $J_{xx} = J_{yy} = J_{zz} = 1$ and $J_{xy} = J_{yx}$. Other coupling parameters are zero. The temperature $T = 0$. Number of spins $N = 20$ (solid lines) and $N = 24$ (lines with boxes). The left panel corresponds to $J_{xy} = 0.1$; the right panel corresponds to $J_{xy} = 0.5$ [see Eq. (12)].

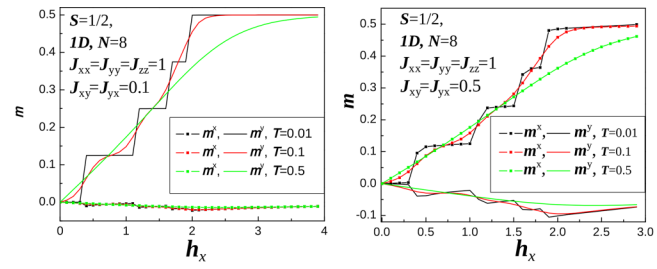



FIG. 9. Spin-1/2 chain with $N = 8$ spins. The dependencies of the magnetic moments $m^x$ (lines with boxes) and $m^y$ (lines) on the magnetic field $h_x$. We use $J_{xx} = J_{yy} = J_{zz} = 1$ and $J_{xy} = J_{yx}$. Other coupling parameters are zero. The left panel corresponds to $J_{xy} = 0.1$ [see Eq. (12)]; the right panel corresponds to $J_{xy} = 0.5$. Temperatures ($k_B = 1$) are $T = 0.01$, 0.1, and 0.5.

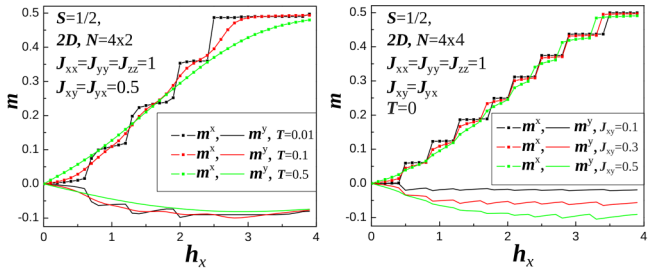



FIG. 10. Spin-1/2 square lattice. The dependencies of the magnetic moments $m^x$ (lines with boxes) and $m^y$ (lines) on the magnetic field $h_x$. We use $J_{xx} = J_{yy} = J_{zz} = 1$ and $J_{xy} = J_{yx}$ [see Eq. (12)]. Other coupling parameters are zero. The left panel corresponds to a square lattice with $4 \times 2$ spins and $J_{xy} = 0.5$. Temperatures ($k_B = 1$) are $T = 0.01$, 0.1, and 0.5. The right panel corresponds to a square lattice with $4 \times 4$. $J_{xy} = 0.1$, 0.3, and 0.5. The temperature is $T = 0$.

related components of the magnetic susceptibility are negative.

We emphasize that, namely, the presence of the special magnetic anisotropy (i.e., $J_{ij} = J_{ji}$, with $i \neq j$, $i, j = x, y, z$, of the special sign) of spin-spin couplings for spin-1/2 systems determines the onset of the magnetic response nonparallel to the applied field and the negative magnetic susceptibility.

### Dzyaloshinskii-Moriya interaction

The antisymmetric Dzyaloshinskii-Moriya exchange (like $S_p^i S_q^j - S_p^j S_q^i$) does not yield such an effect.

The field dependencies of magnetization for one-, two-, and three-dimensional spin systems with antisymmetric Dzyaloshinskii-Moriya exchange are presented in Figs. 12–14. The exchange constants and the temperatures are the same as for Figs. 8–11. The only difference is $J_{xy} = -J_{yx}$. As can be seen, the magnetization component, perpendicular to the applied field, is absent.

In principle, small sizes of the studied clusters for two- and three-dimensional systems can introduce an additional artificial anisotropy. However, one can see that the considered

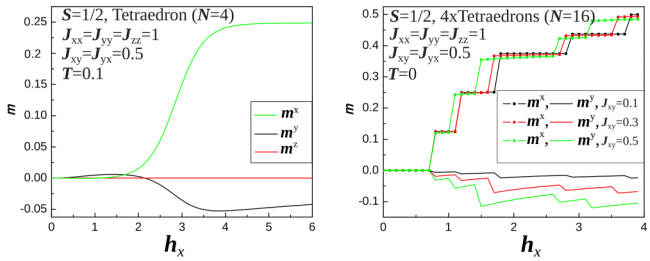



FIG. 11. Spin-1/2 tetrahedron(s). We use $J_{xx} = J_{yy} = J_{zz} = 1$ and $J_{xy} = J_{yx}$. Other coupling parameters are zero. The left panel corresponds to a single tetrahedron ($N = 4$). The dependencies of the magnetic moments $m^{x,y,z} = M^{x,y,z}/g_{x,y,z}\mu_B$ (green, black, and red lines, respectively) on the magnetic filed $h_x$ are shown. We use $J_{xy} = 0.5$ [see Eq. (12)]. The temperature is ($k_B = 1$) $T = 0.1$. The right panel corresponds to a cluster of $4 \times$ tetrahedrons ($N = 16$). The dependencies of the magnetic moments $m^x$ (lines with boxes) and $m^y$ (lines) on the magnetic field $h_x$ are shown. We use $J_{xy} = 0.1$, 0.3, and 0.5. The temperature is $T = 0$.

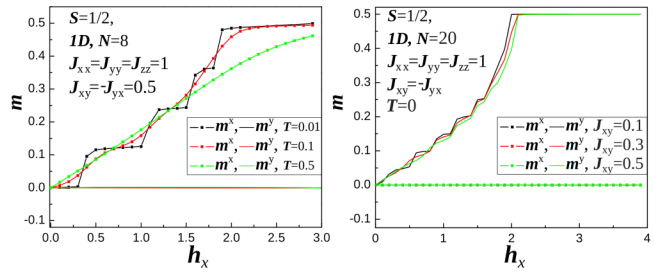



FIG. 12. Spin-1/2 chain. The dependencies of the magnetic moments $m^x$ (lines with boxes) and $m^y$ (lines) on the magnetic field $h_x$. We use $J_{xx} = J_{yy} = J_{zz} = 1$ and $J_{xy} = -J_{yx}$. Other coupling parameters are zero. The left panel corresponds to $N = 8$. $J_{xy} = 0.5$. The temperatures ($k_B = 1$) are $T = 0.01$, 0.1, and 0.5. The right panel corresponds to $N = 20$ with $J_{xy} = 0.1$, 0.3, and 0.5. The temperature is $T = 0$.

effect is present in Figs. 8–11 (with $J_{xy} = J_{yx} \neq 0$) but not present in Figs. 12–14 (with $J_{xy} = -J_{yx} \neq 0$) for the same sizes of studied clusters. Hence, the effect is caused by the intrinsic, not by the artificial anisotropy due to small cluster sizes.

## IV. QUANTUM NATURE OF THE EFFECT

The effect is totally quantum in nature. In systems with the magnetic ordering, which can be described using classical vectors [2], the low symmetric magnetic anisotropy produces different effects. The external magnetic field rotates magnetic moments; however, it does not cause their onset as in paramagnets or low-dimensional spin systems or spin systems with geometric frustrations. Both projections of the magnetic moment (parallel and perpendicular to the field direction) increase with the growth of the external magnetic field. This is why we expect the absence of the effect for infinite low-dimensional quantum spin systems in the ground state, in which magnetic ordering can take place.

Let us consider the magnetically ordered system with the monoclinic magnetic anisotropy. In the simplest case, the energy of the system can be written as

$$E = \frac{A}{2}(M^x M^y + M^y M^x) - \gamma H_x M_x - \gamma H_y M^y, \qquad (13)$$

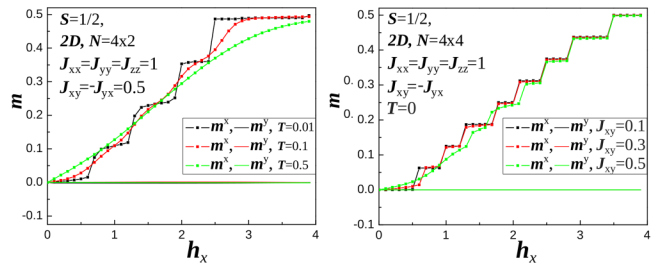



FIG. 13. Spin-1/2 square lattice. The dependencies of the magnetic moments $m^x$ (lines with boxes) and $m^y$ (lines) on the magnetic field $h_x$. We use $J_{xx} = J_{yy} = J_{zz} = 1$ and $J_{xy} = -J_{yx}$. Other coupling parameters are zero. The left panel corresponds to $N = 4 \times 2$ spins and $J_{xy} = 0.5$; temperatures ($k_B = 1$) are $T = 0.01$, 0.1, and 0.5. The right panel corresponds to $N = 4 \times 4$ spins. $J_{xy} = 0.1$, 0.3, and 0.5. The temperature is $T = 0$.

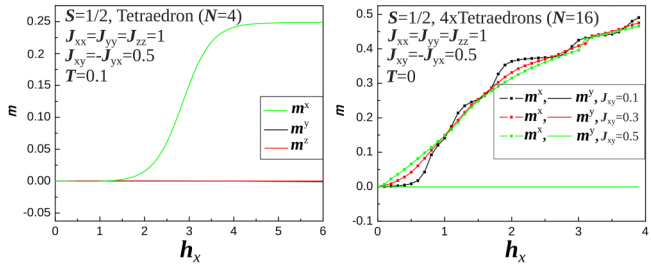



FIG. 14. Spin-1/2 tetrahedron(s). $J_{xx} = J_{yy} = J_{zz} = 1$ and $J_{xy} = -J_{yx}$. Other coupling parameters are zero. The left panel corresponds to a single tetrahedron ($N = 4$). The dependencies of the magnetic moments $m^{x,y,z} = M^{x,y,z}/g_{x,y,z}\mu_B$ (green, black, and red lines, respectively) on the magnetic filed $h_x$. We use $J_{xy} = 0.5$ [see Eq. (12)]. The temperature is ($k_B = 1$) $T = 0.1$. The right panel corresponds to the cluster of 4 × tetrahedrons ($N = 16$). The dependencies of the magnetic moments $m^x$ (lines with boxes) and $m^y$ (lines) on the magnetic field $h_x$. We use $J_{xy} = 0.1$, 0.3, and 0.5. The temperature is $T = 0$.

where $M^{x,y}$ are the components of the magnetization, $H_{x,y}$ are the components of the external magnetic field, $A$ is the parameter of the magnetic anisotropy, and $\gamma$ is the gyromagnetic ratio. Using the parametrization $M^x = M_0 \cos\theta$ and $M^y = M_0 \sin\theta$, the energy can be rewritten as

$$E = \frac{A}{2}M_0^2 \sin 2\theta - \gamma H_x M_0 \cos\theta - \gamma H_y M_0 \sin\theta. \qquad (14)$$

Minimization of the energy with respect to $\theta$ yields for $H_x = 0$

$$M^x = \frac{M_0}{4}\left(h_y^2 - \sqrt{h_y^2 + 8AM_0}\right),$$
$$M^y = \sqrt{M_0^2 - (M^x)^2}, \qquad (15)$$

where $h_y = \gamma H_y$. The magnetic field behavior of the components of the magnetization is shown in Fig. 15.

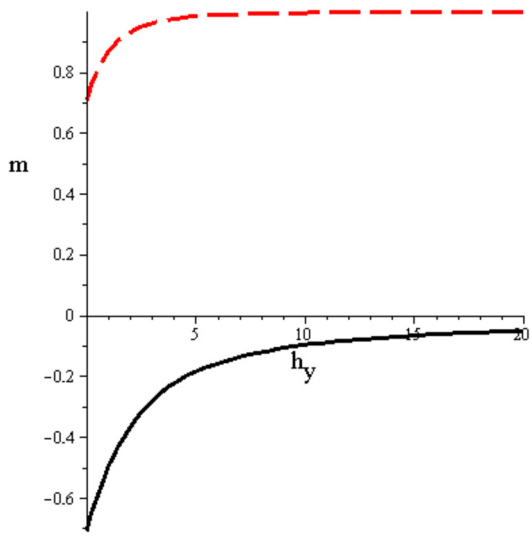



FIG. 15. The dependence of the components of the magnetization $m^{x,y} = M^{x,y}/M_0$ ($m^y$: black solid line; $m^x$: red dashed line) of the magnetically ordered system with the monoclinic magnetic anisotropy $A = 1$ on the magnetic field $h_y = \gamma H_y$.

One can see that the magnetization is rotated under the action of the magnetic field. Obviously, absolute values of both components of the magnetization increase with the growth of the magnetic field.

## V. SUMMARY

In summary, we have studied quantum spin systems with low symmetries of the magnetic anisotropic properties. We have shown that the low symmetry produces very special effects of their magnetic characteristics. Namely, magnetic moments induced by the external magnetic field can be nonparallel to the direction of the field. Also, we have shown that the components of the magnetic susceptibility of such systems can be negative (i.e., the diamagnetic behavior) for a large range of the field and temperature. We have shown that the effect is generic for a wide class of quantum spin systems, including paramagnets, low-dimensional quantum spin systems, and frustrated spin systems like quantum spin ices. The origin of the effect is totally quantum. One can regulate the values of the effective crystalline electric fields by strains or by the application of the external electric field. The effect can be of principal importance for the technological application of quantum systems, e.g., in quantum computing, where low symmetries of distribution of qubits or qudits and their environment can yield special features of their response to the gates. Another principal area of interest is in the creation of metamaterials. Obviously, negative refractive index implies a negative real part of the dynamical susceptibility. The static susceptibility, considered in our work, is the limit (for frequency tends to zero) of the real part of the dynamical susceptibility. It is very difficult to believe that the real part of the dynamical susceptibility changes its sign only at zero frequency. Hence, the negative static susceptibility implies the negative real part of the dynamical susceptibility and, therefore, the negative refractive index. For example, the space symmetry and the values of crystal field parameters for rare-earth metallic borates [32,33] indicate the possibility of existence of a negative index for electromagnetic waves, namely, in the terahertz frequency range, which is determined by the values of crystalline electric fields in many low-symmetric rare-earth based paramagnets. For instance, for the compound $SmAl_3(BO_3)_4$, the values of the crystalline electric field are $B_2^0 = 282\,\mathrm{cm}^{-1} = 406\,\mathrm{K}$, $B_4^0 = -900\ \mathrm{cm}^{-1} = -1256\,\mathrm{K}$, and $C_4^3 = -1520\ \mathrm{cm}^{-1} = -2189\,\mathrm{K}$, i.e., most of transitions between levels are in the terahertz (infrared) frequency range.

## ACKNOWLEDGMENTS

A.A.Z. acknowledges the support from the Deutsche Forschugsgemeinschaft via the SFB 1143. V.V.S. acknowledges the support from the Wolfgang Pauli Institut within the WPI thematic program "Mathematics-Magnetism-Materials (2024/2025)".

## DATA AVAILABILITY

No data were created or analyzed in this study.

[1] R. M. White, *Quantum Theory of Magnetism* (Springer-Verlag, New York, 1983).

[2] L. D. Landau and E. M. Lifshitz, *Electrodynamics of Continuous Media* (Pergamon Press, Oxford, 1984).

[3] M. Tinkham, *Group Theory and Quantum Mechanics* (McGraw-Hill, New York, 1964).

[4] See, e. g., A. A. Zvyagin, *Quantum Theory of One-Dimensional Spin Systems* (Cambridge Scientific Publishers, Cambridge, 2010).

[5] A. A. Zvyagin and V. V. Slavin, Intersite spin nematic ordering in the spin-1/2 chain system, Phys. Rev. B **109**, 104409 (2024).

[6] N. Bloembergen, Linear Stark effect in magnetic resonance spectra, Science **133**, 1363 (1961).

[7] B. Lüthi, *Physical Acoustics in the Solid State* (Springer-Verlag, Berlin, 2005).

[8] W. Law, Paramagnetic resonance in solids, in *Supplement 2 of Solid State Physics: Advances in Research and Applications*, edited by F. Seitz and D. Turnbull (Academic Press Inc., NY, 1960).

[9] J. S. Gardner, M. J. P. Gingras, and J. E. Greedan, Magnetic pyrochlore oxides, Rev. Mod. Phys. **82**, 53 (2010).

[10] J. T. Chalker, Geometrically frustrated antiferromagnets: Statistical mechanics and dynamics, in *Introduction to Frustrated Magnetism: Materials, Experiments, Theory*, edited by C. Lacroix, P. Mendels, and F. Mila (Springer, Berlin, 2011).

[11] A. A. Zvyagin, New physics in frustrated magnets: Spin ices, monopoles, etc., Low Temp. Phys. **39**, 901 (2013) [Fiz. Nizk. Temp. **39**, 1159 (2013)].

[12] J. G. Rau and M. J. Gingras, Frustrated quantum rare-earth pyrochlores, Annu. Rev. Condens. Matter Phys. **10**, 357 (2019).

[13] J. Villain, Insulating spin glasses, Zeit. Phys. B **33**, 31 (1979).

[14] M. Nielsen and I. Chuang, *Quantum Computation and Quantum Information* (Cambridge University Press, Cambridge, 2000).

[15] J. Stolze and D. Suter, *Quantum Computing: A Short Course From Theory to Experiment* (Wiley-VCH, Berlin, 2004).

[16] K. T. Lin, H. Lin, T. Yang, and B. Jia, Structured graphene metamaterial selective absorbers for high efficiency and omnidirectional solar thermal energy conversion, Nat. Commun. **11**, 1389 (2020).

[17] V. O. Cheranovskii, V. V. Slavin, E. V. Ezerskaya, A. L. Tchougrèeff, and R. Dronskowski, Magnetic properties of quasi-one-dimensional crystals formed by graphene nanoclusters and embedded atoms of the transition metals, Crystals **9**, 251 (2019).

[18] L. A. Pastur, V. V. Slavin, and A. A. Krivchikov, Ground state of one-dimension repulsing particles on disordered lattice, Int. J. Mod. Phys. C **25**, 1450028 (2014).

[19] D. Schurig, J. J. Mock, B. J. Justice, S. A. Cummer, J. B. Pendry, A. F. Starr, and D. R. Smith, Metamaterial electromagnetic cloak at microwave frequencies, Science **314**, 977 (2006).

[20] S. S. Islam, M. R. I. Faruque, and M. T. Islam, A near zero refractive index metamaterial for electromagnetic invisibility cloaking operation, Materials **8**, 4790 (2015).

[21] L-W Li, Y-N Li, T. S. Yeo, J. R. Mosig, and O. J. F. Martin, A broadband and high-gain metamaterial microstrip antenna, Appl. Phys. Lett. **96**, 164101 (2010).

[22] J. V. de Almeida, G. L. Siqueira, M. M. Mosso, and C. A. F. Sartori, Mu-negative metamaterials seen as band-limited non-Foster impedances in inductive power transmission systems, J. Microw. Optoelectron. Electromagn. Appl. **18**, 492 (2019).

[23] A. Kumar, N. Kumar, and S. C Gupta, Gain improvement of microstrip patch antenna using negative permeability metamaterial reflecting surface, J. Electr. and Electr. Engin. **9**, 53 (2014).

[24] P. Kumar, T. Ali, and M. M. Manohara Pai, Electromagnetic metamaterials: A new paradigm of antenna design, IEEE Access **9**, 18722 (2021).

[25] X. Xue *et al.*, CMOS-based cryogenic control of silicon quantum circuits, Nature (London) **593**, 205 (2021).

[26] C. H. Yang, R. C. C. Leon, J. C. C. Hwang, A. Saraiva, T. Tanttu, W. Huang, J. C. Lemyre, K. W. Chan, K. Y. Tan, F. E. Hudson, *et al.*, Operation of a silicon quantum processor unit cell above one kelvin, Nature (London) **580**, 350 (2020).

[27] L. M. K. Vandersypen and M. A. Eriksson, Quantum computing with semiconductor spins, Phys. Today **72**(8), 38 (2019).

[28] I. Hansen, A. E. Seedhouse, S. Serrano, A. Nickl, M. Feng, J. Y. Huang, T. Tanttu, N. D. Stuyck, W. H. Lim, F. E. Hudson, *et al.*, Entangling gates on degenerate spin qubits dressed by a global field, Nat. Commun. **15**, 7656 (2024).

[29] A. Abragam and B. Bleaney, *Electron Paramagnetic Resonance of Transition Ions* (Clarendon Press, Oxford, 1970).

[30] L. K. Aminov, B. Z. Malkin, and M. A. Teplov, Chapter 150 Magnetic properties of nonmetallic lanthanide compounds, Handb. Phys. Chem. Rare Earths **22**, 295 (1996).

[31] S. B. Lee, S. Onoda, and L. Balents, Generic quantum spin ice, Phys. Rev. B **86**, 104412 (2012).

[32] A. A. Zvyagin and V. V. Slavin, Governing of the piezoelectric effect by external fields and strains, Sci. Rep. **14**, 18335 (2024).

[33] V. V. Slavin, A. A. Zvyagin, G. A. Zvyagina, and V. G. Piryatinskaya, Magnetic field effect on the electric permittivity of rare-earth aluminium borates, Low Temp. Phys. **50**, 481 (2024) [Fiz. Nizk. Temp. **50**, 530 (2024)].